Electronic Supplementary Material (ESI) for Journal of Materials Chemistry A.

PdFe alloy nanoparticles supported on nitrogen-doped carbon nanotubes for electrocatalytic upcycling of poly(ethylene terephthalate) plastics into formate coupled with hydrogen evolution

Heng Zhang,[a,b] Zhenzhen Liu,[a,b] Huaimeng Li,[a] Zhen Fu,[a] Guofeng Zhang,[a] Haimin Zhang,[a,b] Guozhong Wang,[a,b] and Yunxia Zhang*[,a,b]

[a] *Key Laboratory of Materials Physics, Centre for Environmental and Energy Nanomaterials, Anhui Key Laboratory of Nanomaterials and Nanotechnology, Institute of Solid State Physics, Hefei Institutes of Physical Science, Chinese Academy of Sciences, Hefei 230031, China.*

[b] *University of Science and Technology of China, Hefei 230026, P. R. China*

* Correspondence Author. Email: yxzhang@issp.ac.cn
Fax: +86-551-65591434; Tel: +86-551-65592145

S1. Experimental section

S1.1. Chemicals and materials

Carbon nanotubes (CNTs, diameter = 60−100 nm) were purchased from Shenzhen Nanotech Port Co., Ltd (China). Ferric acetylacetonate ($Fe(acac)_2$) and NaI were obtained from Alfa Aesar. The commercial Pt/C (20 wt%) and RuO_2 was obtained from Johnson Matthey. Polyvinyl pyrrolidone (PVP), N, N-dimethylformamide (DMF), and KOH were all used as received if not mentioned. Carbon cloth (CC) was obtained from Hongshan District, Wuhan Instrument Surgical Instruments (China). Before using, CC was pretreated with a HNO_3 aq. solution, and then sonicated in acetone, H_2O and CH_3CH_2OH for 30 min, respectively.

S1.2. Material characterizations

The phase and crystalline structure of as-prepared samples were identified by X-ray diffraction (XRD, X'Pert Pro Super, Philips Co., The Netherlands) with Cu Kα radiation (1.5478 Å). The morphology characterization of catalysts was collected on scanning electron microscopy (FE-SEM, SU8020, Hitachi) and a high-resolution transmission electron microscope (HRTEM, JEM-2010, JEOL, Japan). X-Pay photoelectron spectroscopy (XPS) measurements were performed on Thermo Scientific ESCALAB 250, while all of the binding energies were calibrated using C1s peak (284.8 eV). Fourier transform infrared (FT-IR) spectra were recorded on Thermo Nicolet NEXUS FT-IR spectrophotometer at room temperature. The content of metal elements in the catalysts was measured using an inductively coupled plasma atomic emission spectrometer (ICP-AES, ICP-6300, Thermo Fisher Scientific). The H_2 content was determined by online gas chromatography (GC9790Plus, FULI INSTRUMENTS) thermal conductivity detector (TCD).

S1.3. Electrochemical measurements

Unless otherwise specified, all electrochemical measurements were conducted at room temperature using CHI 660E electrochemical analyzer (CHI Instruments, Shanghai, China) in a conventional three-electrode system. A platinum wire was used as a counter electrode for EGOR and a graphite road for HER. The reference electrode for all measurements was Hg/HgO. The catalyst supported the carbon cloth was directly used as the working electrode with a geometric area of 0.25 cm^2. The inks were obtained by sonicating the mixture containing catalysts, i.e. 5 mg of catalyst, 475 μL of ethanol, 475 μL of water, and 50 μL of 5 wt% Nafion for 30 min. The ink mixture was coated on the CC surface with a loading of 1 mg/cm^2. The 1 M KOH aqueous solution was used as the electrolytes, and all the polarization curves were recorded at a scan rate of 5 mV/s unless specifically indicated.

Electrochemical impedance spectroscopy (EIS) tests were carried out at a frequency ranging from 0.1 Hz to 100 kHz with AC amplitude of 10 mV. Furthermore, the potentials were converted to RHE scale according to the equation: E(vs. RHE) = E (vs. Hg/HgO) + 0.059*pH +0.098 V, where the pH value of 14 for 1.0 M KOH.

S1.4. Product analysis

To determine the products of EG oxidation and calculate Faradaic efficiencies, the long-term bulk electrolysis was carried out in a three-electrode system at the constant potential of 1.35 V (vs. RHE) in 10 mL 1.0 M KOH with 0.3 M ethylene glycol under vigorous stirring at room temperature. The electrolyte solutions were collected after approximately 2 h electrolysis and then analyzed by nuclear magnetic resonance (NMR) spectrometer. ^1H NMR spectra were recorded on an AVANCE 400 (Bruker), in which 500 μL electrolyte was added with 50 μL D_2O and 30 L dimethyl sulfoxide

(DMSO) used as an internal standard. The quantity of products in the samples was calculated by Eq. (1)

$$m_{product} = \frac{I_{product} \times N_{DMSO} \times M_{product}}{I_{DMSO} \times N_{product} \times M_{DMSO}} \times m_{DMSO} \times n \quad (1)$$

where $I_{product}$ is the integral of product peak; $N_{product}$ is the numbers of proton or carbon corresponding to product peak; $M_{product}$ is the molar mass of product; m_{DMSO} is the mass of DMSO; n = 50 mL/500 μL = 100.

The selectivity (%) and yield (%) of formate can be determined by the following Eq. (2) and (3), respectively.

$$Selectivity(\%) = \frac{N(formate\ yield)}{2N(consumed\ EG)} \times 100\% \quad (2)$$

$$Yield = \frac{N(formate\ yield)}{2N(initial\ EG)} \times 100\% \quad (3)$$

The Faraday efficiency (%) of the product formation can be determined by the following Eq. (4)

$$FE(\%) = \frac{N(formate\ yield)}{toal\ charge\ passed/3 \times 96485} \times 100\% \quad (4)$$

The Faradaic efficiency (FE) of HER catalysts is defined as the ratio of the amount of experimentally determined H_2 (n_e) to that of the theoretically expected H_2 (n_t) based on the reported method [1]:

$$FE = \frac{n_e}{n_t} \quad (5)$$

Theoretical amount of H_2 was calculated by applying Faraday Law:

$$n_t = \frac{JAt}{2F} \quad (6)$$

Where J is current density, A is electrode area, t is time in second, 2 is number of electron, and F is faraday constant (96,485 C/mol). The Faradaic efficiency is conducted under galvanostatic

electrolysis at a current density of −20 mA/cm^2 over a period of 50 min. Furthermore, the evolved H_2 was quantified by online gas chromatography using the water drainage method. The experimentally determined volume of H_2 was very close to that of the theoretical value.

S1.5. PET and real-world plastic bottle pretreatment

2 g of PET was pretreated in a 50 mL solution of 10 M KOH at 60 ^oC for 8h, and the resulting suspension was used for electroreforming in the PdFe/N-CNTs//PdFe/N-CNTs pair-electrolysis system.

S1.6. Terephthalic acid (TPA) separation

After electrolysis of PET hydrolysate, sulfuric acid was used to adjust the PH to < 3 as an acidifier for TPA precipitation and regeneration through filtration. The resulting liquid stream was then concentrated and crystallized to solid K_2SO_4.

S1.7. ECSA calculation

Electrochemical capacitance measurements were used to determine the active surface area of each catalyst. To estimate the electrochemical active surface area of the electrocatalysts, double-layer capacitance (C_{dl}) was considered in the non-faradaic region (−0.654 ~ −0.714 V vs. RHE) of CVs recorded at different scan rates of 10, 20, 30, 40, 50 and 60 mV/s. Then, plotting the double-layer charging current at −0.684 V vs. scan rate yielded a linear slope. Finally, the ECSA was obtained by dividing C_{dl} by the specific capacitance of the electrode material. Generally, the specific capacitance for flat surface electrodes was 0.06 mF/cm^2.

S1.8. Turnover frequency calculations

To calculate the per-site turnover frequency (TOF), we used the following formula according to

previous reports[1].

$$TOF\ per\ site = \frac{\#\ Total\ Hydrogen\ Turn\ Overs/cm^2 geometric\ area}{\#\ Surface\ Sites\ /cm^2\ geometric\ area}$$

The number of total hydrogen turn overs is calculated from the current density using the following equation:

$$\#_{H_2} = \left(j\frac{mA}{cm^2}\right)\left(\frac{1C\ s^{-1}}{1000\ mA}\right)\left(\frac{1\ mol\ e^-}{96485.3\ C}\right)\left(\frac{1\ mol\ H_2}{2\ mol\ e^-}\right)\left(\frac{6.022\ \times 10^{23}\ H_2\ molecules}{1\ mol\ H_2}\right) = 3.12\ \times 10^{15}\frac{H_2/s}{cm^2}\ per\ \frac{mA}{cm^2}$$

The total number of effective surface sites was calculated based on the following equation:

$$\frac{\#\ Surface\ sites}{cm^2\ geometric\ area} = \frac{\#\ Surface\ sites\ (flat\ standard)}{cm^2\ geometric\ area} \times Roughness\ factor$$

Here the roughness factor (Rf) can be determined by the double-layer capacitance (C_{dl}). The surface sites of 2×10^{15} for the flat standard electrode was used for our calculation according to previous results[2]. Thus, the number of surface active sites for the PdFe/N-CNTs catalyst is estimated to be 5.43×10^{18} surface sites/cm^2. Therefore, in 1 M KOH solution, the TOF per site for the PdFe/N-CNTs catalyst at $_{100}$ is calculated as follows: $0.046\ \frac{H_2/\ s}{surface\ site}$

S1.9. Mass Activity

The mass activity of the composite was calculated according to the following formula:

Mass Activity (MA) = Catalytic Activity (CA) / Mass of Catalyst (MC)

where catalytic activity is the rate of the target reaction (e.g., current density, reaction rate)

S1.10. Theoretical calculation

In order to simulate the loading of nanoscale PdFe particles on the surface of CNTs, a 6-atom nanocluster (Pd_xFe_{6-x}) was chosen. On the basis of the Woolf structure, the face-centered cubic palladium metal was more inclined to the cubic octahedral geometric structure, and Pd_6 was the smallest of the octahedral "magic numbers".[3,4] Since the size of the CNT in the experiment was

larger than that of PdFe nanoparticles, some studies have shown that the curvature of the CNT carrier has little effect. Therefore, the CNT carrier is was approximated as a graphene sheet to reduce the complexity of the model. The model added a 15 Å vacuum layer along the Z axis to eliminate the interaction between the upper and lower surfaces. The model used a Monkhorst K-point grid with a 3 × 3 × 1 grid. All geometric optimizations were performed using the conjugate gradient algorithm implemented in CASTEP. The projector augmented wave (PAW) method was employed to treat the core electrons, and the generalized gradient approximation (GGA) of Perdew-Burke-Ernzerhof (PBE) to describe the exchange-correlation energy.[5,6] The Kohn-Sham wave functions were expanded with a cutoff energy of 400 eV. The calculated binding energy (E_{ads}) was evaluated based on the following equation:

$$\Delta G_{ads} = E_{sur+adsorbate} - E_{sur} - E_{adsorbate}$$

where $E_{sur+adsorbate}$, E_{sur}, and $E_{adsorbate}$ are the obtained energies for the slab system containing the adsorbate, the energy of the slab, and the energy of the adsorbate in a vacuum, respectively. Here, 'adsorbate' refers to chemisorbed ethylene glycol or H_2O species.

1. L. Yu, I.K. Mishra, Y. Xie, H. Zhou, J. Sun, J. Zhou, Y. Ni, D. Luo, F. Yu, Y. Yu, S. Chen, Z. Ren, *Nano Energy,* 2018, **53**, 492-500.

2. J. Kibsgaard, C. Tsai, K. Chan, J.D. Benck, J.K. Nørskov, F. Abild-Pedersen, T.F. Jaramillo, *Energy Environ. Sci.,* 2015, **8**, 3022-3029.

3. D. Chen, Z. Pu, R. Luo, P, Ji, P. Wang, J. Zhu, C. Lin, H.-W. Li, X. Zhou, Z. Hu, F. Xia, J. Wu and S. Mu, *Adv. Energy Mater.,* 2020, **10,** 2000814.

4. V. N. Popov, *New J. Phys.* 2004, **6**, 17.

5. W. Miehle, O. Kandler, T. Leisner and O. Echt,, *J. Chem.Phys*.,1989, **91**, 5940-5952.

6. J. P. Perdew, K. Burke and M. Ernzerhof, *Phy. Rev. Lett.* 1996, **77**, 3865.

S3. Techno-economic analysis

S3.1. Costs:

S3.1.1. Material costs

Material costs: 1 ton PET (500 $/t), 1.4 ton KOH (850 $/t), 2 ton water (0.22 $/t), 1.2 ton H_2SO_4 (148 $/t)

$$Material\ cost = 1868\ \$$$

S3.1.2. Electricity costs:

The total charge required for electro-reforming per ton of PET can be calculated as follows:

$$Q = \frac{mass\ of\ ethylene\ glycol\ (g) \times F \times N}{Molar\ mass\ of\ ethylene\ glycol\ (g/mol) \times\ FE}$$

Where Q is the total charge, n is the mole of EG (1 ton of PET), F is the Faraday's constant (96485) and N is the number of electron transfer (6), FE (85%) is the faradaic efficiency of formate production from PET electro-reformin.

The power required to maintain electrolysis process can be calculated as follows, assuming that the cell potential is 1.45 V, f is the capacity factor (0.8).

$$P = \frac{U \times Q}{3600\ f}$$

$$Electricity\ cost = P \times Price$$

S2.1.3. Separation costs:

The separation costs are 50 % of electricity costs. Therefore, the electricity cost can be calculated as:

Electricity costs = Electrolyser electricity cost + Hydrolysis and Separation electricity

The price of electricity is assumed to be 0.07 $/kWh.

S3.1.4. Miscellaneous costs:

In the PET plastic electrocatalytic upcycling process, miscellaneous costs including capital costs, installation costs, operating costs, and maintenance costs are 1165 $/ton PET according to the reference.

S3.2. Output products:

The products of this process include terephthalic acid (TPA), formic acid (FA) and K_2SO_4. Per ton of PET as raw material can obtain 906 kg TPA (951 $/ton), 436 kg FA (1479 $/ton), 2215 kg K_2SO_4 (887 $/ton), and 0.0359 ton H_2 (1900 $/ton). Therefore, the product value can be calculated as:

Total output product values = Cost of TPA × Mass of PET obtained + Cost of FA × Mass of FA obtained + Cost of K_2SO_4 × Mass of K_2SO_4 obtained Cathode HER to produce formic acid, which has a 99.3 % faradaic efficiency.

$$Mass\ of\ H_2\ from\ HER\ at\ cathode = \frac{Q \times Molar\ mass\ of\ H_2}{NF}$$

Where N takes the value 2 since H_2O reduced to H_2 is a two-electron transfer process.

S3.3. Potential profit:

Therefore, the total income of electrolysis per ton of PET can be calculated as follows: Total profit per ton of PET = Product value per ton of PET-Total costs per ton of PET. Total profit = Product value − total cost = 3539.4 − 3127.5 = 411.9 $

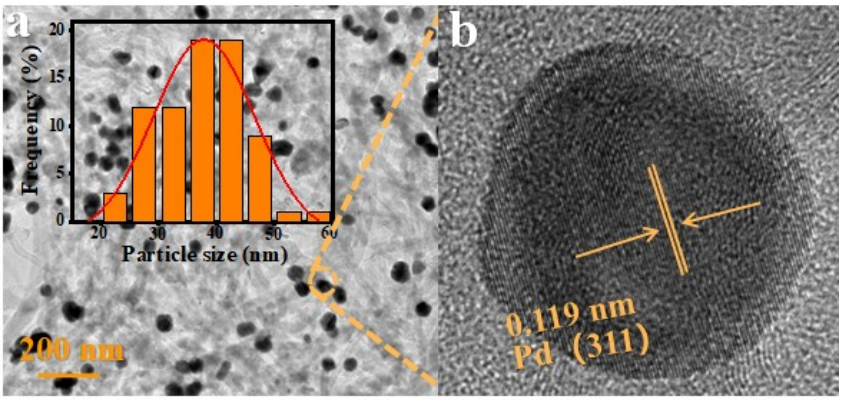

Fig. S1 (a) TEM and (b) HRTEM image of Pd/CNTs catalysts.

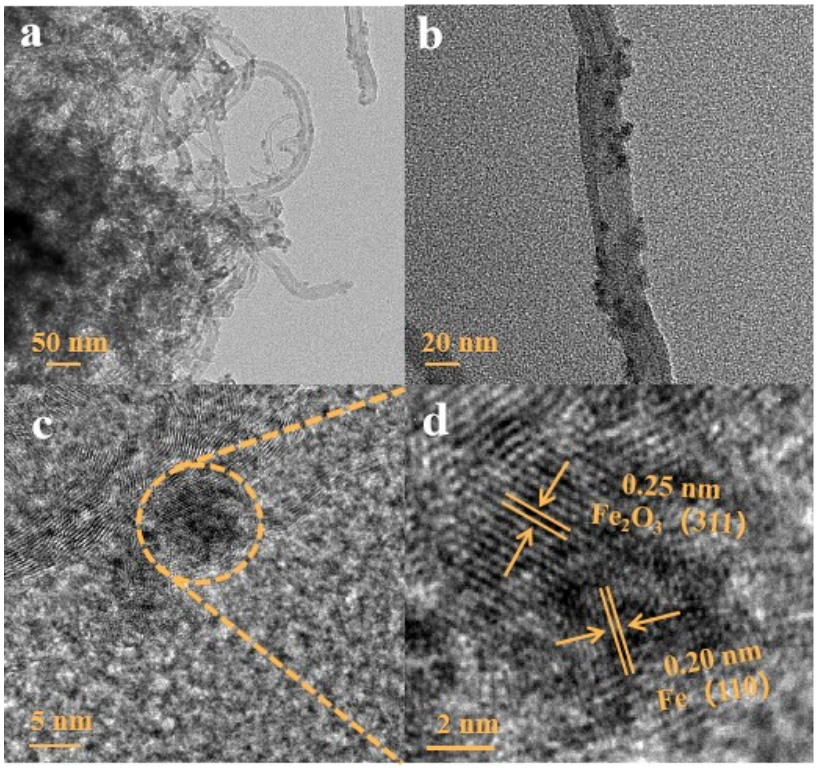

Fig. S2 TEM (a, b) and HRTEM (c, d) images of Fe/CNTs catalysts.

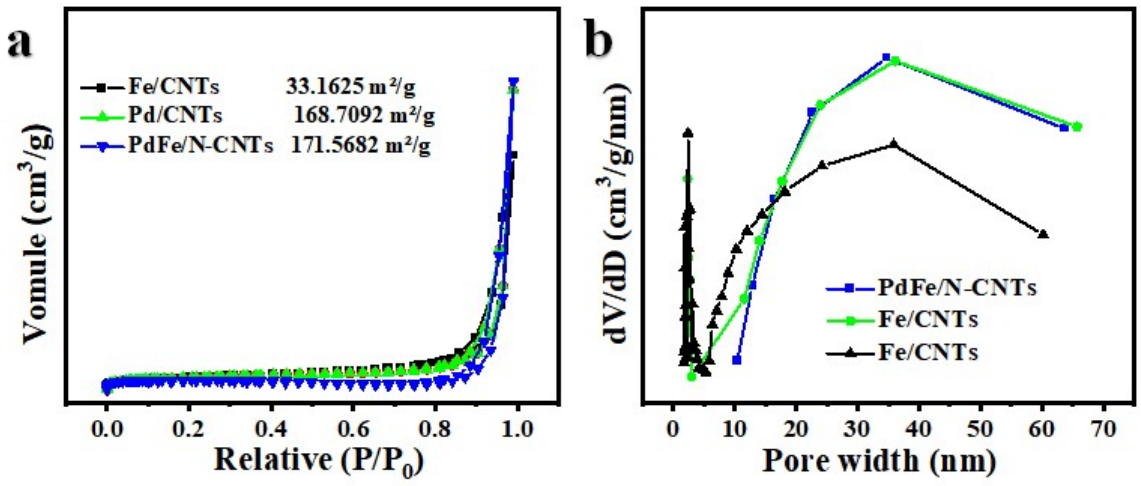

Fig. S3 (a) Nitrogen adsorption-desorption isotherms and (b) pore size distribution of the samples.

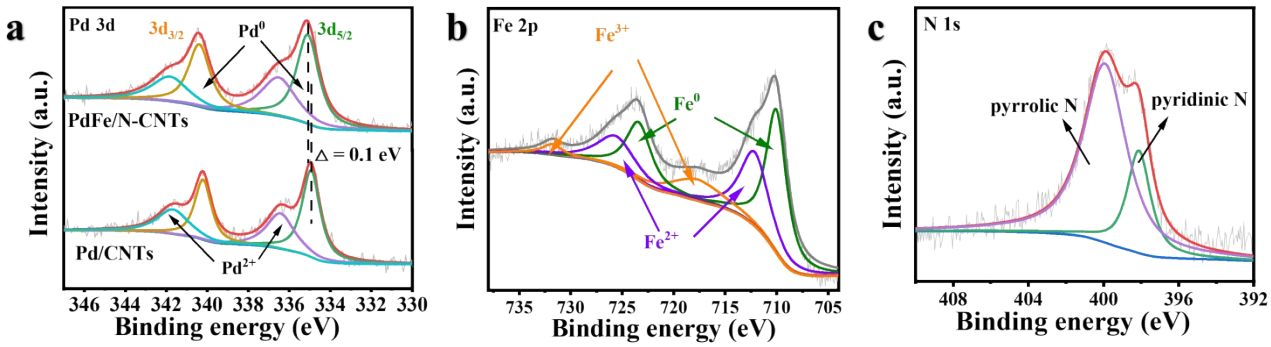

Fig. S4 The high-resolution XPS spectra: (a) Pd 3d in PdFe/N-CNTs and Pd/CNTs; (b) N 1s in PdFe/N-CNTs; (c) Fe 2P in Fe/CNTs.

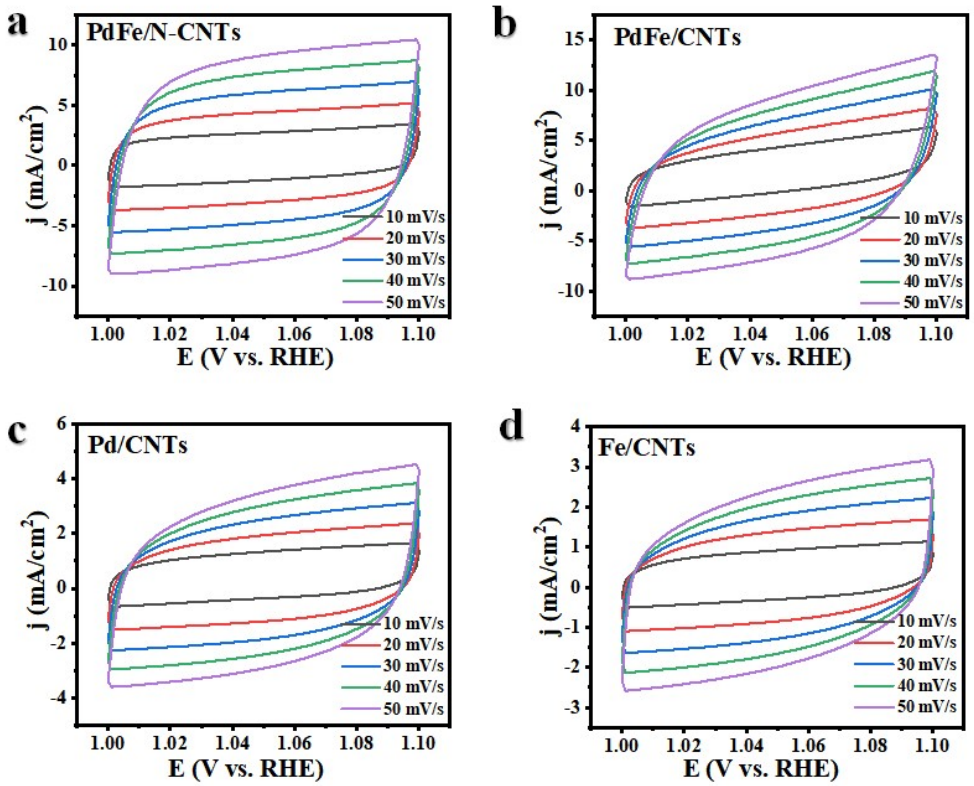

Fig. S5 CV curve of various electrodes recorded at different scan rates of 10, 20, 30, 40, and 50 mVs^{-1} for (a) PdFe/N-CNTs, (b) PdFe/CNTs, (c) Pd/CNTs and (d) Fe/CNTs.

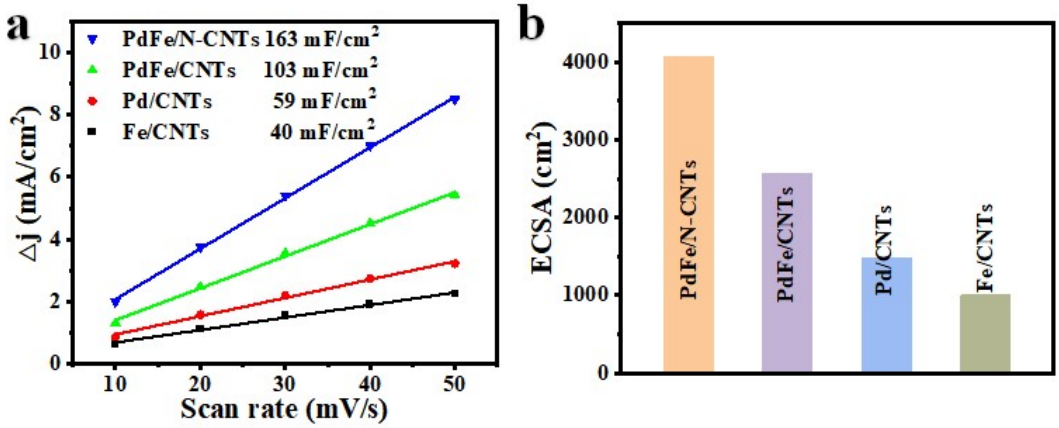

Fig. S6 The double layer capacity C_{dl} and ECSA of PdFe/N-CNTs, PdFe/CNTs, Pd/CNTs and Fe/CNTs.

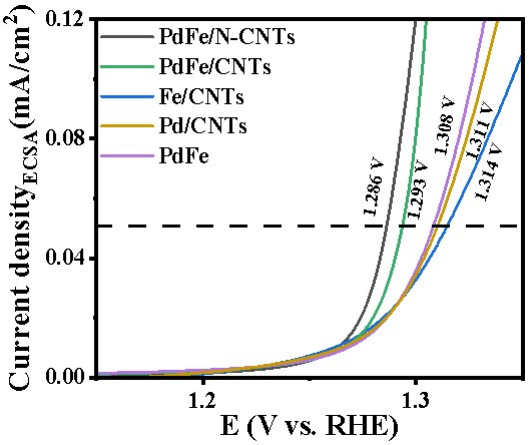

Fig. S7 The normalized EGOR LSV curves based on ECSA.

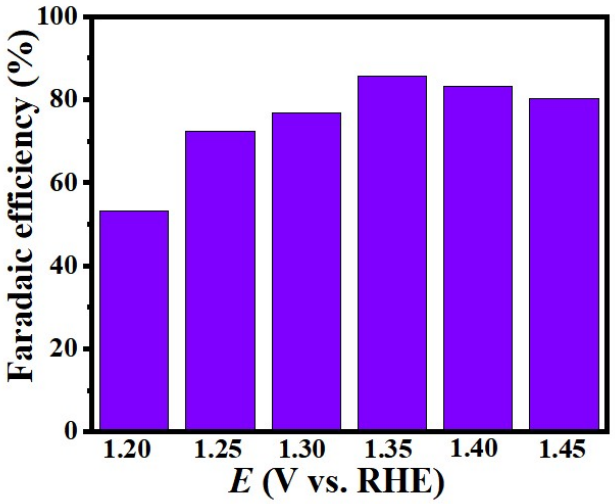

Fig. S8 Faradaic efficiencies for formate production at various potentials.

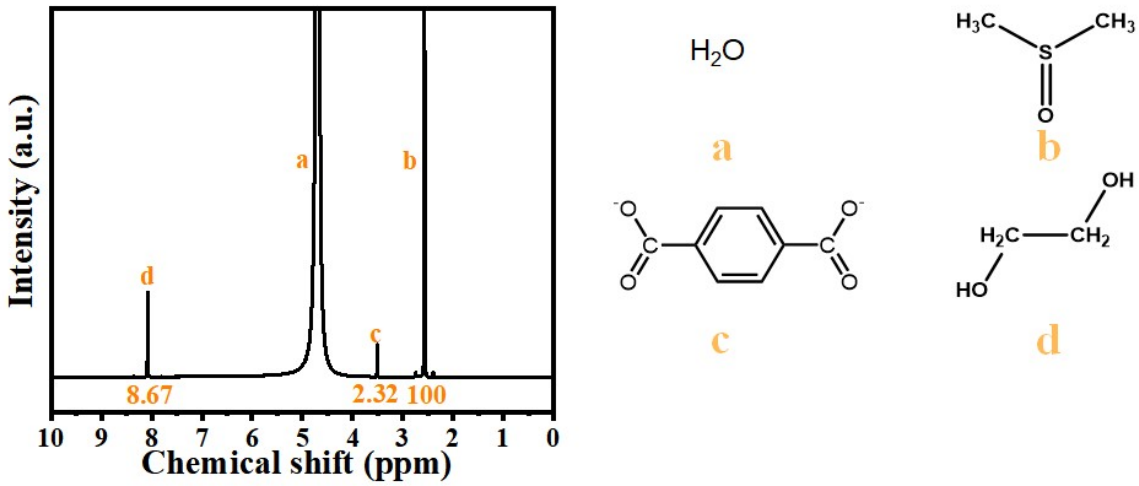

$$m_{EG} = \frac{I_{EG} \times N_{DMSO} \times M_{EG}}{I_{DMSO} \times N_{EG} \times M_{DMSO}} \times m_{DMSO} \times n = \frac{2.32 \times 6 \times 62.068}{100 \times 4 \times 78.12} \times 33 \times 20 = 18.25\ mg$$

$$m_{formate} = \frac{I_{formate} \times N_{DMSO} \times M_{formate}}{I_{DMSO} \times N_{formate} \times M_{DMSO}} \times m_{DMSO} \times n = \frac{8.67 \times 6 \times 46.03}{100 \times 1 \times 78.12} \times 33 \times 20 = 202.3\ mg$$

$$Selectivity_{formate}\ \frac{N_{formate} = \frac{m_{formate}}{M_{formate}}}{2N_{Consumed\ EG} = \frac{m_{EG}}{M_{EG}}} \times 100\% = \frac{\frac{202.3}{46.03}}{2 \times \frac{183.7 - 18.25}{62.068}} = 82.44\ \%$$

$$FE_{formate}\ \frac{n \times N_{formate} \times F}{Total\ passed\ charge\ (C)} \times 100\% = \frac{3 \times 0.0044 \times 96485}{1463.23} = 87.04\ \%$$

Fig. S9 ^{1}H NMR spectra after EGOR on PdFe/N-CNTs at 1.35 V.

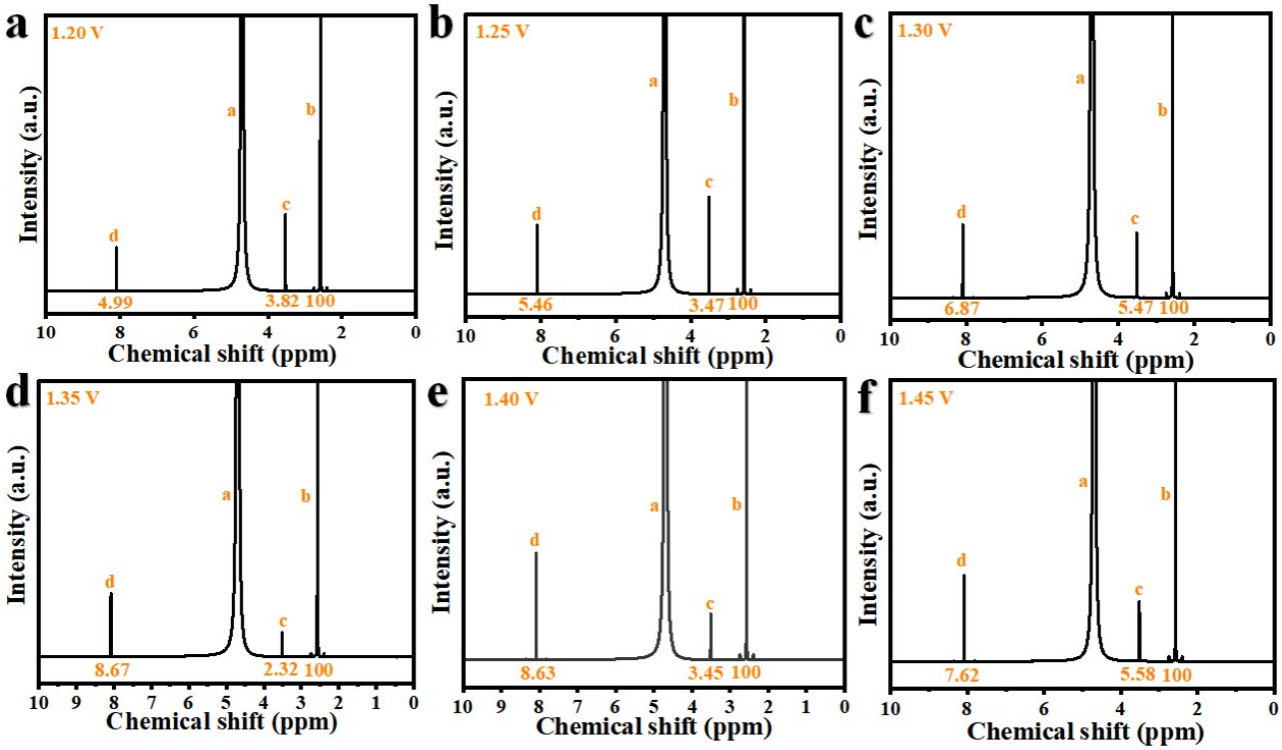

Fig. S10 ^{1}H NMR spectra after EGOR on PdFe/N-CNTs in 1.20–1.45 V.

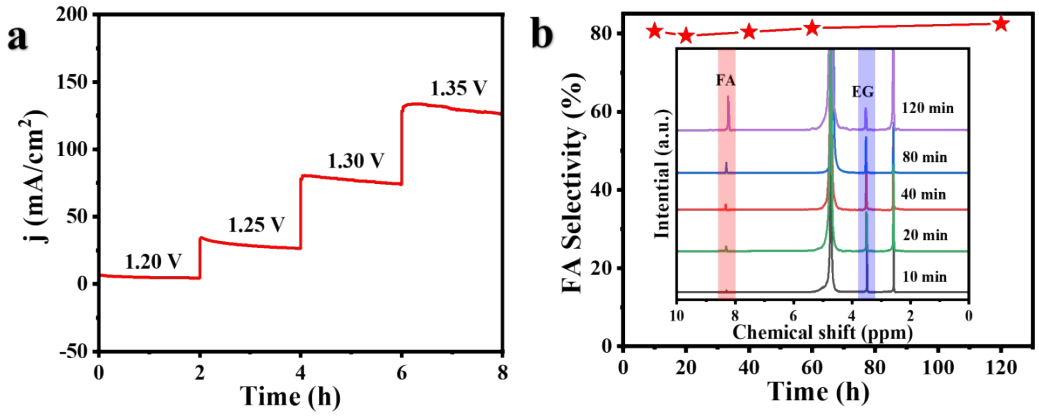

Fig. S11 (a) Stability test of PdFe/N-CNTs electrode toward EGOR at different petentials; (b) FA selectivity as a function of time.

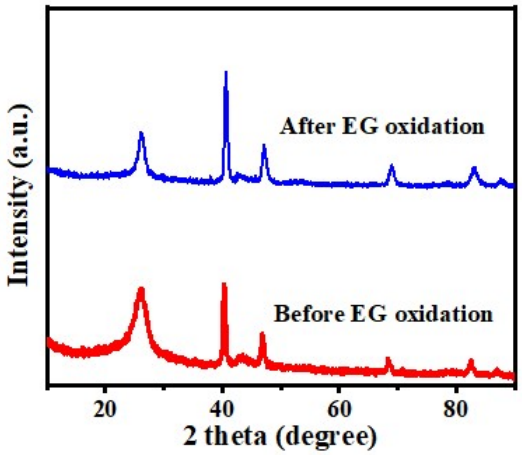

Fig. S12 XRD pattern of PdFe/N-CNTs before and after EG oxidation.

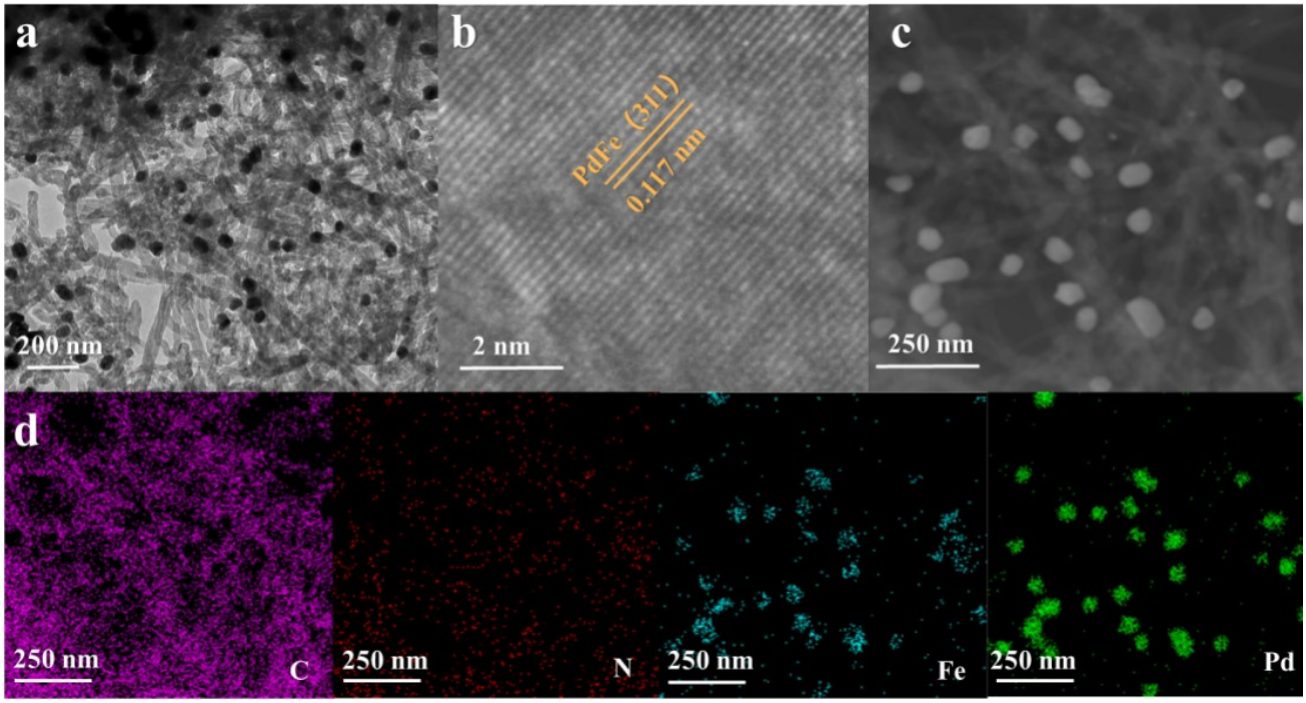

Fig. S13 PdFe/N-CNTs images after EGOR: (a) TEM, (b) HRTEM, (c) HAADF-STEM, and (d) the corresponding elemental mappings of Pd, Fe, N, C.

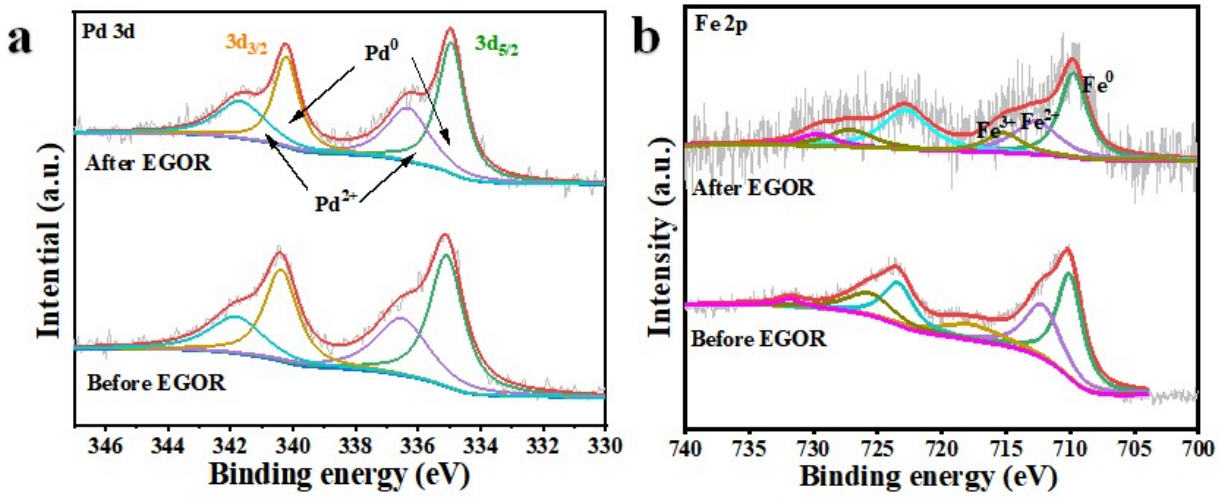

Fig. S14 XPS spectra of PdFe/N-CNTs after EGOR test: (a) Pd 3d; (b) Fe 2P.

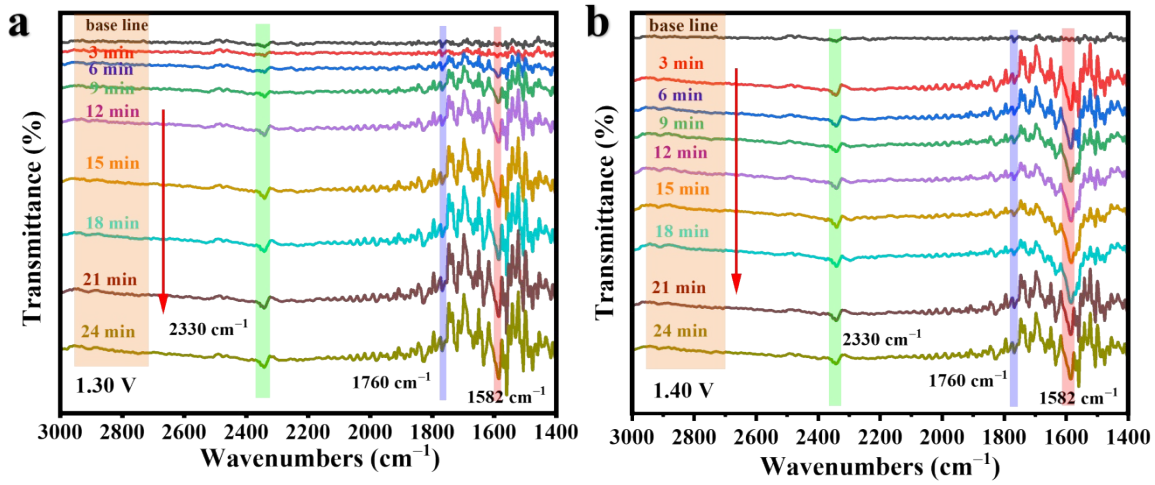

Fig. S15 Time-dependent *In-situ* FTIR of PdFe/N-CNTs at varying potentials in 1 M KOH + 0.3 M EG: (a) 1.30 V and (b) 1.40 V.

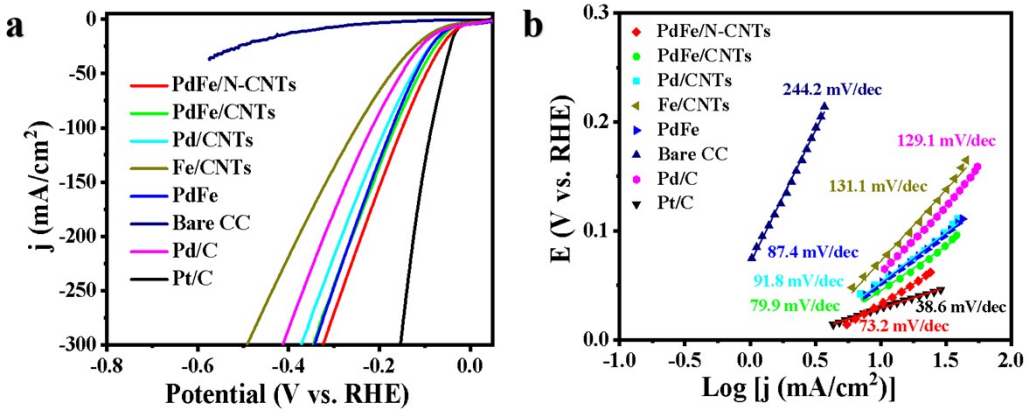

Fig. S16 (a) HER polarization curves of PdFe/N-CNTs, PdFe/CNTs, Pd/CNTs and Fe/CNTs catalysts, and (b) the corresponding Tafel plots.

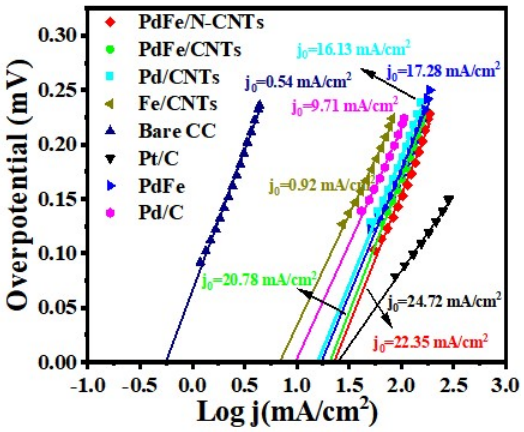

Fig. S17 The exchange current densities of Bare CC, Fe/CNTs, Pd/C, Pd/CNTs, PdFe, PdFe/CNTs, PdFe/N-CNTs and Pt/C.

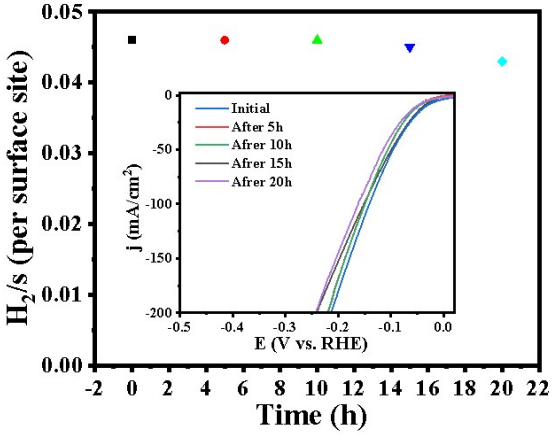

Fig. S18 The TOF values of PdFe/N-CNTs catalyst with time (the inset: LSV curve over time).

Fig. S19 EIS spectra of Fe/CNTs, Pd/C, Pd/CNTs, PdFe, PdFe/CNTs and PdFe/N-CNTs.

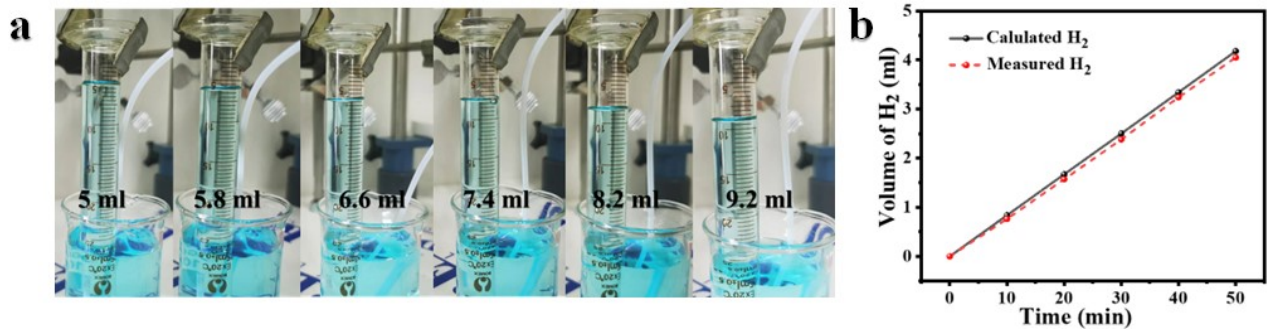

Fig. S20 (a) Amount of H2 generation for PdFe/N-CNTs in 1M KOH at time interval of 10 min; (b) Calculated and measured amount of H_2 as a function of time.

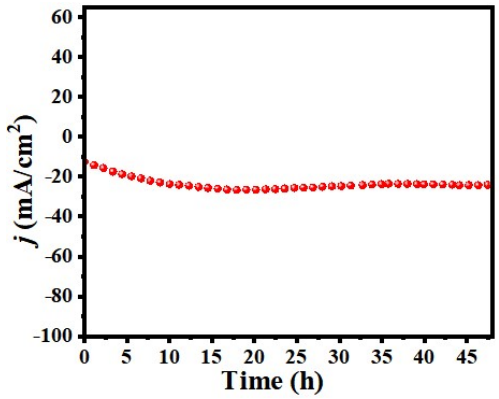

Fig. S21 Chronopotentiometry curve of PdFe/N-CNTs during HER process.

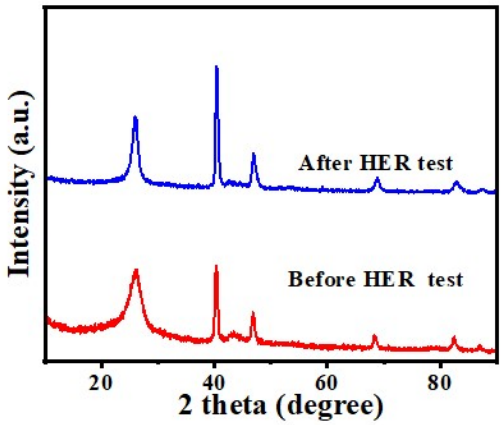

Fig. S22 XRD pattern of PdFe/N-CNTs after HER durability test.

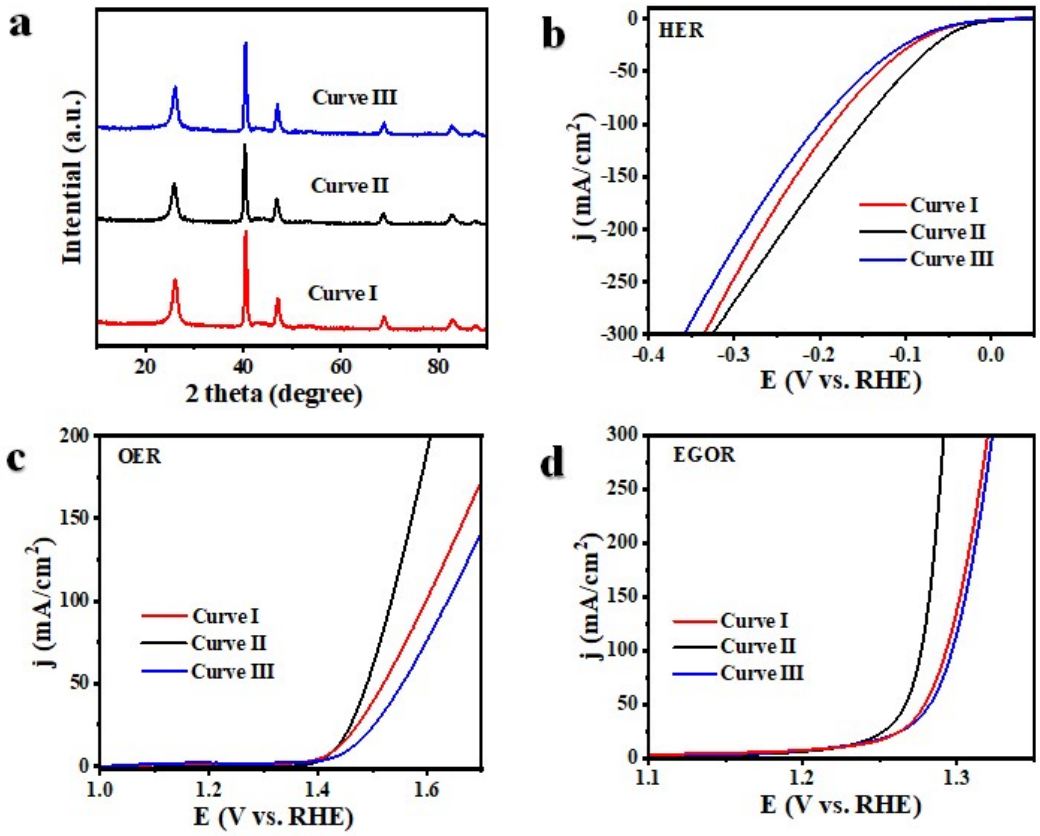

Fig. S23 XRD patterns, b) HER, c) OER, and d) EGOR polarization curves of various PdFe/N-CNTs catalysts with different Pd/Fe ratios (Curve I: Pd/Fe=1:1; Curve II: Pd/Fe=1:2; Curve III: Pd/Fe=1:3).

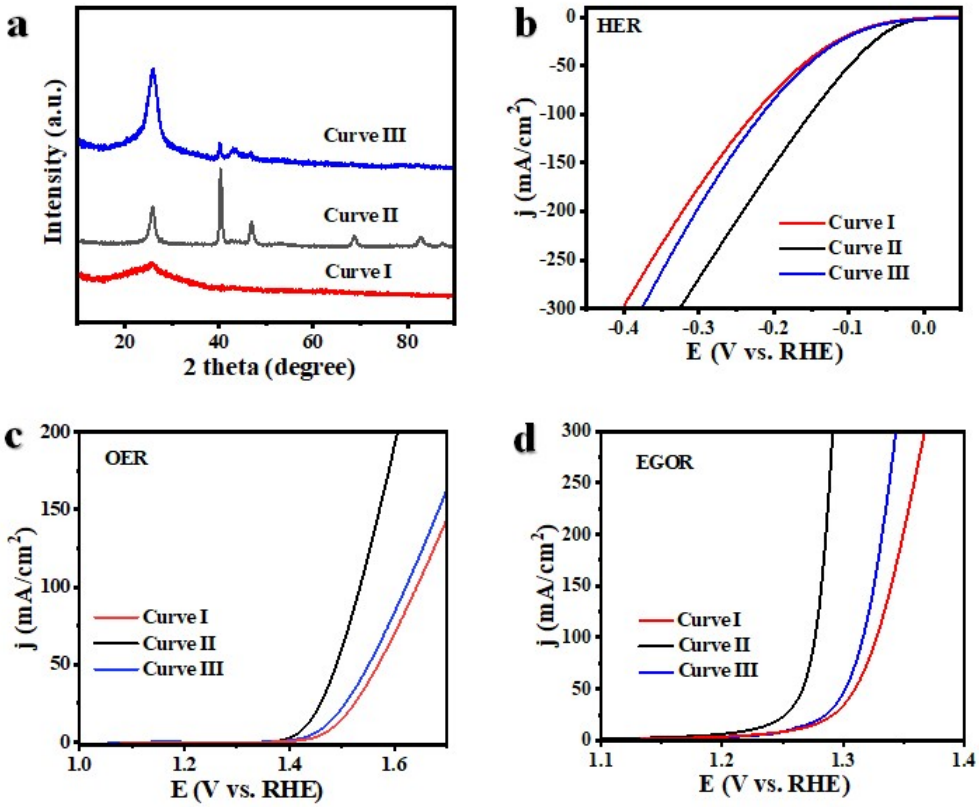

Fig. S24 (a) XRD patterns, (b) HER, (c) OER, and (d) EGOR polarization curves of various PdFe/N-CNTs catalysts under different pyrolysis temperature (Curve I: 300 °C; Curve II: 500 °C; Curve III: 700 °C).

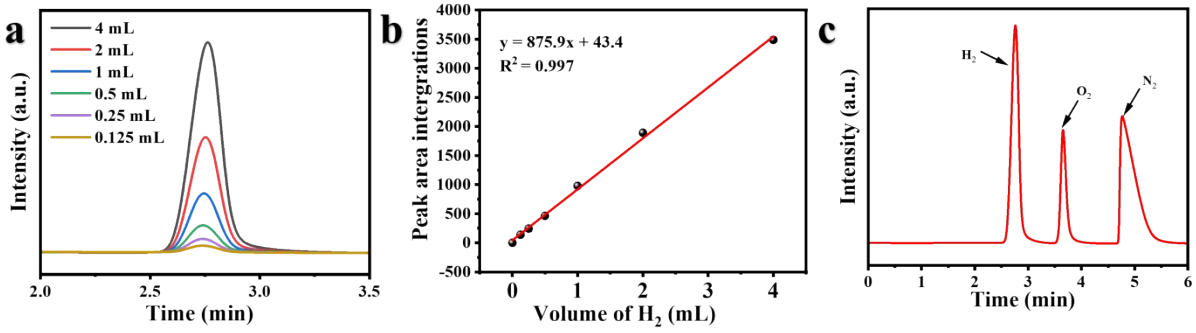

Fig. S25 (**a**) Gas chromatography spectra of the various H_2 volume; (**b**) The calibration curve used for calculation of H_2 volume; (**c**) Gas chromatography spectra of H_2 volume at 1.45 V.

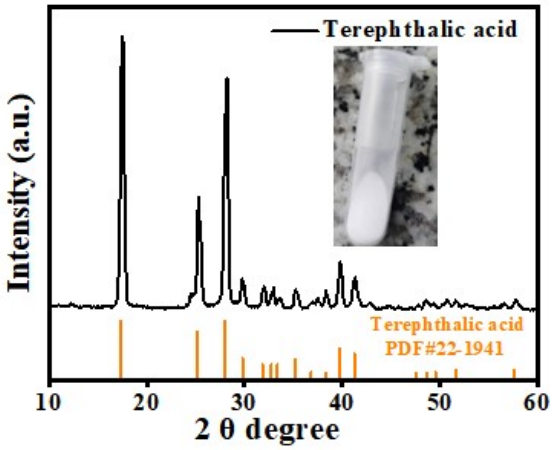

Fig. S26 XRD pattern of the recovered TPA (inset: digital photograph of the recovered TPA powder).

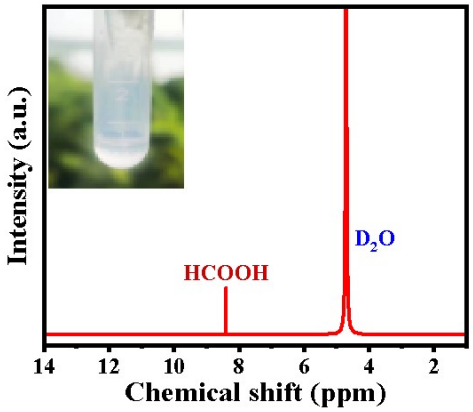

Fig. S27 ^{1}H NMR spectrum of formic acid (inset: digital photograph of formic acid).

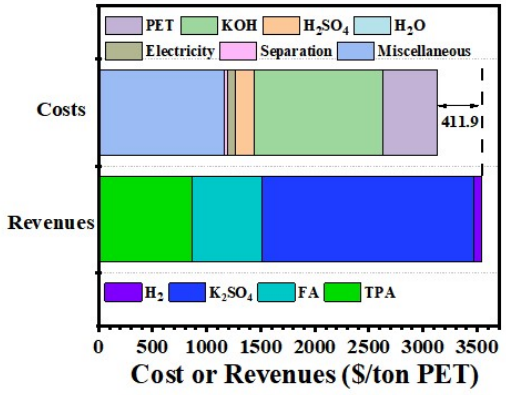

Fig. S28 Technoeconomic analysis of this electro-reforming process. Assuming 100% of PTA and

100% of K_2SO_4 are recycled.

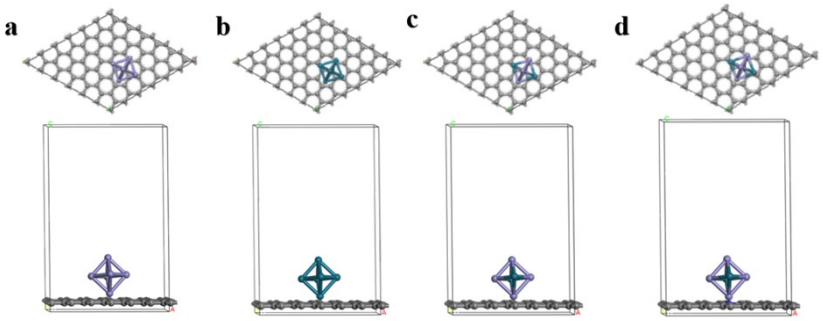

Fig. S29 Theoretical modes of (a) Fe/CNTs, (b) Pd/CNTs (c) PdFe/CNTs and (d) PdFe/N-CNTs.

Table S1 A summary of the performance on a 10,100-mA/cm^2 scale for the electrocatalytic oxidation of EG in alkaline electrolytes in available literature.

Catalysts	Electrolyte	Potential$_{OER}$ $j_{10,100}$ (V *vs.* RHE)	Potential$_{EGOR}$ $j_{10,100}$ (V *vs.* RHE)	Potential $_{OER-EGOR}$ j_{100} (V *vs.* RHE)	FE(%)	Ref.
PdFe/N-CNTs	**1 M KOH +0.3 M EG**	**1.43, 1.54**	**1.22, 1.28**	**260**	**87**	**This work**
$CuCo_2O_4$/NF	1 M KOH + 0.06 M EG	1.57, 1.72	1.23, 1.47	250	86	Green Chem., 24 (2022) 6571-6577.
NiO@C/CC	1 M KOH + 1 M EG	j_{50} =1.96, 2.06	J_{50} = 1.66, 1.82	240	–	Adv. Energy Mater. 10 (2020) 2001397.
OMS-Ni_1-CoP	1 M KOH + 0.5 M EG	1.45, 1.60	1.30, 1.42	180	93.2	Appl. Catal. B: Environ. 316 (2022) 316, 121667.
Co-Ni_2P/NF	1 M NaOH + 2 g/L PET	/1.52	1.24, 1.37	150	85	Sustain. Energ. Fuels, 6 (2022) 4916-4924.
$Bi_{0.13}Co_{2.83}O_4$-550	1 M KOH + 1 M EG	1.63, 1.72	1.34, 1.42	300	-	Sustain. Energ. Fuels, 6 (2022) 4916-4924.
Ni_3N-$Ni_{0.2}M_{0.8}$NNWs/CC	1 M KOH + 0.3 M EG	1.51, 1.65	1.32, 1.43	220	-	J. Energy Chem. 72 (2022) 432-441.
$NiCo_2O_4$/CFP	1 M NaOH + 0.06 M EG	1.55, /	1.31, 1.47	/	85	ACS Catal. 12 (2022) 6722-6728.

Table S2 HER comparison in 1.0 KOH with the recently reported literatures.

Materials	Tafel slope (mV dec^{-1})	η_{10} / mV	Reference
PdFe/N-CNTs	**70.4**	**32**	**This work**
Pd ND/DR-MoS_2	41	40	*J. Mater. Chem. A* 4 (2016) 4025-4031.
Pd/MOFDC	78	35	*RSC Adv.* 10 (29) (2020) 17359-17368.
Pd/$NiFeO_x$	78	76	*Adv. Funct. Mater.* 31 (51) (2021) 2107181.
Pd-e-NiCo-PBA-C	67	147	*Adv. Funct. Mater.* 31 (10) (2020) 2008989.
RMoS_2-Pd	35.9	86	*ACS Appl. Mater. Interfaces* 11(45) (2019) 42094
Pd/Mo_3N_2	88	65	*Phy. Chem. Chem. Phy.* 224 (2) (2022) 771-777.
Pd/G/ZnO/NF	46.5	31	*RSC Adv.* 9 (58) (2019) 33814-33822
$PdCuRu_{7.6}$	52	31	*J. Mater. Chem. A* 7 (35) (2019) 20151-20157.
$Pd_{86}B_{14}$/C	36.6	38	*Chem. Eng. J.* 433 (2022) 133525.
Pd NN	–	110	*ACS Appl Mater Interfaces* 9 (45) (2017) 39303-39311.
RhPd-H-NS/C	35.7	40	*J. Am. Chem. Soc.* 142 (7) (2020) 3645-3651.
PdCu NSs	124	106	*Small* 13 (12) (2017) 1602970.
Ni@$Ni(OH)_2$/Pd/rGO	70	76	*J. Power Sources* 352 (2017) 26-33.
Pd–Pt-S	31	71	*ACS Appl Mater Interfaces* 9 (21) (2017) 18008-18014.
$NiCo_2S_4$/Pd	70	83	*ACS Appl Mater Interfaces* 10 (26) (2018) 22248-22256.
PdRuTeNRs	61.6	37	*Nanoscale* 14 (40) (2022) 14913-14920.
PdPtCuNiP	–	32	*Adv. Funct. Mater.* 31 (38) (2021) 2101586.

Table S3 Performance comparison of hybrid electrolysis coupled with EG oxidation reactions in recent reports and this work.

Anode	Electrolyte	Cathode	techno-economic analysis	Cell voltage (V)	Reference
PdFe/N-CNTs	PET hydrolysate	PdFe/N-CNTs	411.9	1.54@100mA/cm^2 1.68@500mA/cm^2	**This work**
$CuCo_2O_4$/NF	PET hydrolysate	Pt/NF	614	1.56V@100mA/cm^2	Green Chem. 24 (2022) 6571-6577.
$Mn_{0.1}Ni_{0.9}Co_2O_{4-\delta}$ RSFs/CFP	PET hydrolysate	Pt sheet	226	1.42V@50mA/cm^2	J. Hazar. Mater. (2023) 131743.
$NiCo_2O_4$/CFP	PET hydrolysate	SnO_2/CC	557	1.90V@20mA/cm^2	ACS Catal. 12 (2022) 6722-6728.
Co-Ni_2P/NF	PET hydrolysate	Co-Ni_2P/NF	-	1.43V@10mA/cm^2	Sustain. Energy Fuels. 6 (2022) 4916.
$CoNi_{0.25}P$/NF	PET hydrolysate	$CoNi_{0.25}P$/NF	350	1.80V@500mA/cm^2	Nat. Commun. 12 (2021) 4679.
Co,Cl-NiS	PET hydrolysate electrolysis and conventional water electrolysis (2 M KOH)	Co,Cl-NiS	-	1.51@100mA/cm^2 1.55@200mA/cm^2	Nano-Micr. Lett. 15 (1) (2023) 210.

Note: j: current density; -: no relevant values are given in the articles.